# Chapter 4

# Thermal desorption and time-dependent adsorption of oxygen on Pd(100)


## Abstract

We have studied the thermal desorption and time-dependent adsorption of $O_2$ on Pd(100) using TPD and the King and Wells technique for various kinetic energies and surface temperatures. Time-dependent adsorption measurements indicate initial $O_2$ dissociation for all surface temperatures between 100 and 600 K. Below 200 K, molecular oxygen also adsorbs on the atomic oxygen overlayer for incident energies between 0.056 and 0.38 eV. Subsequent heating of the combined $O/O_2$ overlayer leads to unexpected high atomic oxygen coverages, comparable to those obtained at high incident energies and high surface temperatures. For adsorption above 200 K, both thermal energy from the substrate and kinetic energy in the gas phase reactant increase the obtained maximum oxygen coverage. We interpret this result to indicate that kinetic energy of $O_2$ is dissipated by local heating of substrate phonons during the dissociation process. The reaction energy and kinetic energy locally heat the surface and may cause nucleation of high-coverage PdO structures.


---

This chapter is based on: A. den Dunnen, L. Jacobse, S. Wiegman, and L.B.F. Juurlink, *in preparation*.

## 4.1 Introduction

Palladium is used as a catalyst material for various oxidation and reduction reactions. A well known example is the CO oxidation reaction in the three-way catalytic converter, where breaking the oxygen-oxygen bond is an important step. The dissociative adsorption and recombinative desorption of $O_2$ on Pd(100) has been extensively studied experimentally and theoretically[35–40,42,62–68].

In chapter 3, we have shown that the oxygen dissociation reaction on Pd(100) proceeds mostly via a direct mechanism. At low energy, a dynamical precursor also contributes to the reactivity and steering causes the high absolute reactivity. At low incident energy and in the zero-coverage limit, the transition of $O_{2,\mathrm{phys}}$, $O_{2,\mathrm{chem}}$, and $O_{\mathrm{ads}}$ is gradual and near barrier-free on Pd(100). With increased coverage, trapping into the molecular state also becomes possible, when the oxygen atoms are blocking the nearest neighbor (NN) sites. This is in line with an electron energy loss spectroscopy (EELS) study[31,33] that showed that even though oxygen on the bare Pd(100) surface dissociates at a surface temperature as low as 10 K at low coverage, it is also possible for $O_2$ to adsorb molecularly at higher coverages. Recent DFT calculations[39] also indicate a stable $O_2$ chemisorption well on Pd(100) with pre-adsorbed O-atoms at various coverages.

Density functional theory (DFT) calculations[39] showed that the preferred binding site of O on Pd(100) is the fourfold hollow site. The most facile pathway for $O_2$ dissociation is the pathway, where the flat lying oxygen molecule is centered above the fourfold hollow site. For the minimum energy path, the oxygen dissociates over the two opposite bridge sites. The energy of the dissociated state on the clean surface is lower than that of the molecularly adsorbed state and the reaction energy has been shown to be efficiently coupled into phonons[42]. For a precoverage of 1/8 ML, the energies of the molecular and atomic states are found to be about equal[39]. At a precoverage of 1/4 ML, the energy of the molecularly adsorbed state is lower than that of the dissociated state. Hence, surface oxidation becomes decreasingly exothermic, but DFT calculations indicate that molecular oxygen adsorbed on the $p(2\times2)$ structure (0.25 ML) would still rather dissociate than desorb. Kinetic Monte Carlo (KMC) simulations that take into account the coverage and surface temperature dependencies, show a quasilinear decrease of the normalized sticking coefficient for coverages up to 0.1 ML, almost independent of surface temperature. At surface temperatures above 150 K, the adlayer can equilibrate, so that

an ordered layer with a coverage of 0.25 ML is formed. At a lower surface temperature, the ordering is kinetically limited and a higher coverage of 0.3 ML can be obtained for a dose of 5 L (Langmuir).

Depending on conditions, such as oxygen dose and surface temperature, different overlayer structures can be formed. The chemisorbed $p(2\times2)$ (figure 4.1a) and $c(2\times2)$ (4.1b) structures and reconstructed $p(5\times5)$ (4.1c) and $(\sqrt{5}\times\sqrt{5})R27^\circ$ structures are formed for ideal coverages up to 0.25, 0.50, 0.64, and 0.8 ML, respectively[32,34,36]. Islands of the structures with higher local coverage are formed before completion of the previous structure.

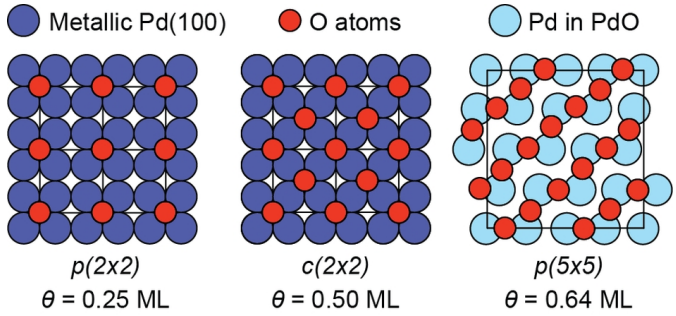


**Figure 4.1:** Representation of oxygen phases on Pd(100) for various coverages, adapted from[36].

Temperature programmed desorption (TPD) studies[34,36,38,68] show a second order, recombinative oxygen desorption peak around 800 to 850 K (the $\alpha$-peak, desorption from a disordered layer) for low coverage. At higher coverage, a shoulder develops on the low temperature side ($\beta$-peak, $c(2\times2)$). A narrow and sharp desorption peak around 620 to 690 K ($\gamma$-peak, decomposition of PdO in the $p(5\times5)$ and/or $(\sqrt{5}\times\sqrt{5})R27^\circ$ structure) is observed at very high coverages. Since this $\gamma$-peak usually develops after dosing at elevated temperatures, the formation of this structure is thought to be activated. Orent and Bader[32] find a peak related to $(\sqrt{5}\times\sqrt{5})R27^\circ$ after dosing at 570 K. Chang and Thiel[36] do not observe this feature even after dosing at 600 K. They only observe a peak related to $p(5\times5)$ after dosing at a surface temperature of 400 K[36]. Stuve and Madix[34] and Zheng and Altman[38] already observe the sharp feature of the $p(5\times5)$ structure after dosing at a temperature between 300 and 350 K. The last group obtained the $(\sqrt{5}\times\sqrt{5})R27^\circ$ structure after dosing 675 L at 525 K, but also after dosing thousands of Langmuir at 400 K. They also report a weak shoulder at 600 K at very high coverages, which

was ascribed to PdO bulk decomposition. The first three states ($p(2\times2)$, $c(2\times2)$, and $p(5\times5)$) can be removed by the presence of CO in the vacuum chamber over a time span of 15 minutes. The $(\sqrt{5}\times\sqrt{5})R27^\circ$ pattern was still visible after 10 hours at 500 K. It was suggested that variations in the minimum surface temperature needed to obtain the $\gamma$-peak may result from differences in the background pressure of CO in the chamber.

It was found before that the nucleation of the reconstructed surface structures depends on the oxygen dose and surface temperature. However, none of the above-mentioned TPD studies include adsorption at different incident energies of the $O_2$ molecule to unravel how the increasing dissociation barrier for increasing O-coverage is surmounted. Also, these studies did not include surface temperatures below 200 K, where a molecular adsorption state seems possible. In this study, we investigate the role of incident energy ($E_i$) and surface temperature ($T_s$) in the range of 100 K to 600 K on the oxygen adsorption and subsequent desorption processes on Pd(100). We use the King and Wells[8] technique and TPD spectroscopy. We show that the sticking probability over time and the formation of the $\gamma$-peak depends on both $E_i$ and $T_s$. A higher oxygen coverage can also be obtained for surfaces with a temperature of 100 K.

## 4.2 Experimental

A detailed description of the ultra-high vacuum (UHV) experimental setup is described in chapter 2. The incident kinetic energy of the supersonic molecular beam was controlled by seeding or antiseeding with helium (Linde, 6.0) or argon (Air Products, 5.7). The kinetic energy of the $O_2$ in our beams was determined by TOF. The sticking probabilities (over time) were determined using the King and Wells technique[8]. Exposure of the crystal to the beam is continued until the exposed surface area has reached a maximum coverage ($\sim$ 5 minutes). Each KW experiment was followed by a TPD experiment, with a heating rate of 2 K/s (for the data shown here or 4 K/s for the old data sets). Besides $^m/_e$ = 32 ($O_2$), $^m/_e$ = 2 ($H_2$), 16 (O), 18 ($H_2O$), 28 (CO or $N_2$), and 44 ($CO_2$) were recorded regularly to check for contamination.

The Pd crystal was cut and polished to expose the (100) plane to $<$ 0.1$^\circ$ accuracy (Surface Preparation Laboratory, Zaandam, The Netherlands). It was extensively cleaned by repeated cycles of $Ar^+$ bombardment (Messer, 5.0; 15 $\mu$A,

5 min.), annealing at a surface temperature of 900 K in an oxygen atmosphere (Messer, 5.0; $3.5{\cdot}10^{-8}$ mbar, 3 min.), and 3 minutes of vacuum annealing at a surface temperature of 1200 K. In between subsequent KW measurements, the crystal was vacuum annealed for 3 minutes at a temperature of 1200 K. Consistency of results was checked by regularly repeating an experiment under identical conditions.

The current produced by our channeltron in the QMS changes over the day, resulting in a decrease in sensitivity and thus a lower intensity of KW and TPD signals. We have corrected our TPD traces with the intensity of the accompanying KW traces to the first experiment of the day. With an additional background correction, this resulted in very reproducible integrated TPD areas for all experiments that were repeated during the day. Figure 4.2 shows the scaling procedure for four experiments dosed at 400 K, with $E_i$ = 0.23 eV, that were repeated during the day (experiment number 3 (black), 9 (blue), 16 (green), and 26 (red)). The top panels (a and b) show the QMS intensity for KW experiments, the middle panels (c and d) show the integrated TPD areas, and the bottom panels (e and f) show the QMS intensity of the TPD experiments. The gray arrows in panel a show the difference in intensity, used to correct the data in the left panels (a, c, and e). The right panels (b, d, and f) show the corrected KW intensities, integrated TPD areas, and corrected TPD intensities. The TPD integrated areas are now the same within $\sim$ 4%. The KW traces are corrected with a double exponential function to correct for small changes in the tail that change over the day.

In order to convert the TPD integrals to a coverage in ML, we compare the oxygen uptake curves from our KW experiments for low $E_i$ and $T_s$ = 200 and 300 K (red solid line) to uptake curves from TPD experiments by Chang and Thiel[36] (green dotted line) and Zheng and Altman[38] (gray dash/dotted line, only at 335 K) (figure 4.3 and 4.4). Zheng and Altman calibrate the coverage by assuming that the saturation coverage of 0.8 ML is reached when the gamma-peak is saturated. The expected $p(2\times2)$ is found at 0.20 ML instead of 0.25 ML in this case. Both groups use background dosing of oxygen, which compares best to our lowest incident energy data. Scaling our low-energy data to a coverage of 0.34 ML results in very comparable uptake curves as previously reported in literature[36,38]. Note that in case our assumption of 0.34 ML is not correct, the coverage values may change, though it will not affect the observed trends or overall conclusions. Chang also reported uptake curves that were determined by Auger spectroscopy (blue dashed lines). However, these curves never follow the same shape as the TPD and KW uptake curves.

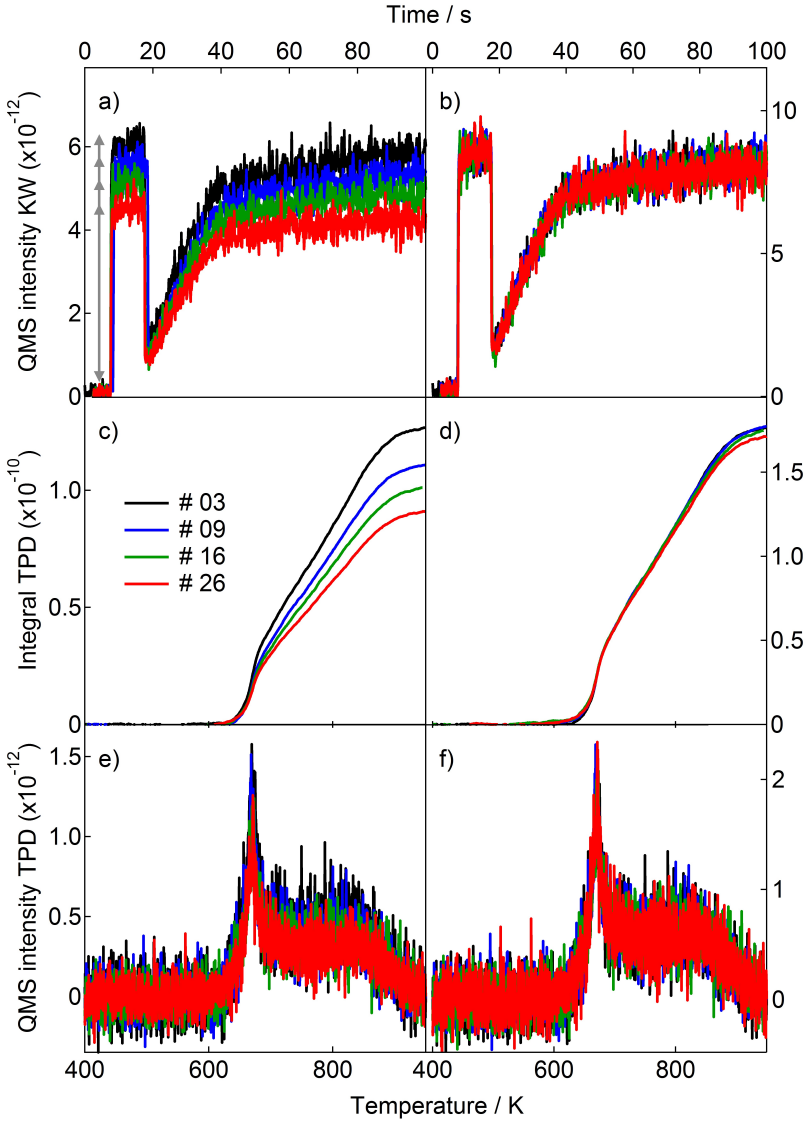


**Figure 4.2:** Scaling of the QMS intensities for 4 experiments dosed at 400 K and 0.23 eV. Top (a and b) panels: QMS intensity of KW experiments. Middle (c and d): TPD integrated areas. Bottom (e and f): QMS intensity TPD experiments. Right (b, d, and f): corrected data.

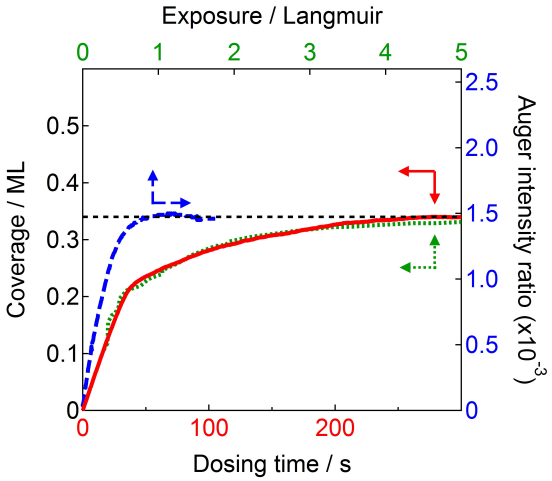


**Figure 4.3:** Oxygen uptake curve for $T_s$ = 200 K for our data (red solid line, $E_i$ = 0.056 eV, integrated KW signal) and data by Chang and Thiel[36] (green dotted line for TPD integrals, blue dashed line for Auger intensity ($T_s$ = 180 K)). Arrows point toward the accompanying axes, the black dashed line indicates 0.34 ML.

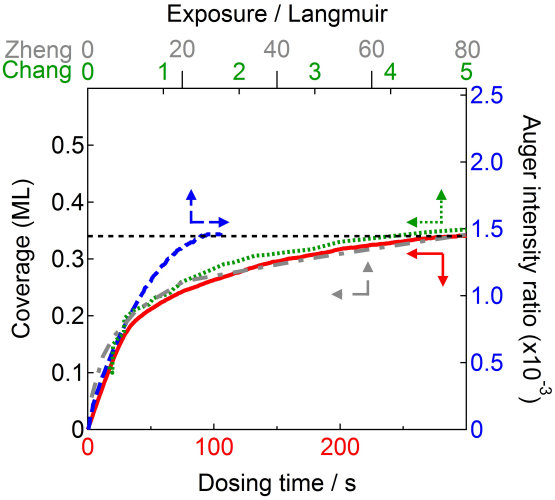


**Figure 4.4:** Oxygen uptake curve for $T_s$ = 300 K for our data (red solid line, $E_i$ = 0.056 eV, integrated KW signal), data by Chang and Thiel[36] (green dotted line for TPD integrals, blue dashed line for Auger intensity), and data by Zheng[38] (gray dash/dotted line for TPD integrals ($T_s$ = 335 K)).

Part of the molecules may already desorb from the surface between closing the beam flag and starting the TPD. However, our integrated KW area shows a trend which is comparable to the integrated area for TPD experiments for various $T_s$ and $E_i$. All beams with different energies have very different intensities and can not directly be compared to each other in KW uptake curves. We have used the least square method to determine the coverage of the KW experiments by comparison to the TPD experiments. We have also compared the TPD shapes of different groups[36,38,68] to our TPD experiments. A coverage of 0.34 ML (only $\alpha$ and $\beta$-peaks and no $\gamma$-peak) for the experiment at 0.056 eV and 200 K seems a reasonable coverage. Other techniques could have confirmed if this assumption is valid. Unfortunately, we were not able to determine the coverage via other techniques. Our low quality LEED device was only able to confirm the (100) orientation of our Pd crystal.

## 4.3 Results

### 4.3.1 Oxygen adsorption

Figure 4.5 shows the sticking traces over time for a) 0.056 eV, b) 0.17 eV, and c) 0.38 eV at $T_s$ = 100 K (blue) and 400 K (gray). At low energy and low temperature, the sticking probability slightly increases over time, stabilizes and eventually decreases exponentially. The trace with a surface temperature of 400 K, also initially increases for almost 10 seconds, as can be seen from the linear fit in this region (black line). After that, it decreases linearly over time. At the highest energy (figure 4.5c), both surface temperatures show nearly identical exponential decreases over time. After 10 seconds, the 100 K trace remains slightly higher than the 400 K trace. At $T_s$ = 100 K and intermediate incident energies (figure 4.5b, only 0.17 eV is shown), the KW trace shows two consecutive inflections. *S* for $T_s$ = 100 and 400 K initially drops nearly linearly. For 100 K, a plateau is reached after approximately 20 s whereas for 400 K a lower plateau is reached after 30 s. For 100 K, the second inflection point occurs at approximately 45 s with an exponential-like drop in *S*. A poorly discernable, but similar inflection and exponential-like drop occurs at 60 s for the 400 K trace.

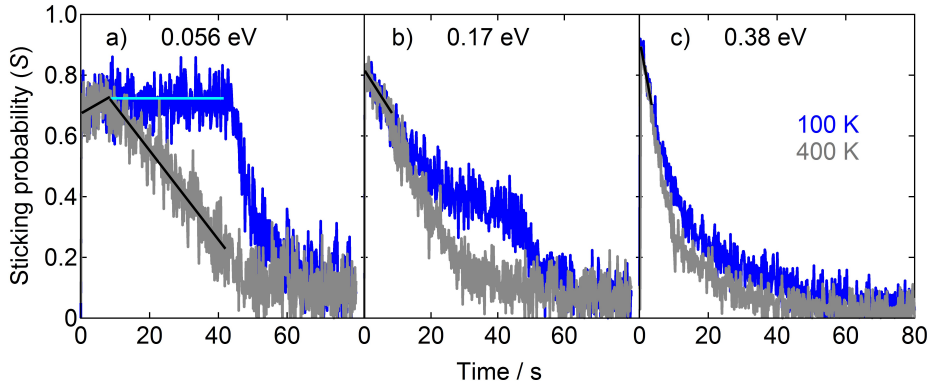


**Figure 4.5:** Sticking traces over time for a) $E_i$ = 0.056 eV, b) 0.17 eV, and c) 0.38 eV at $T_s$ = 100 K (blue) and 400 K (gray). The KW traces are reversed in the y direction, scaled between S = 0 and 1, and shifted in the x direction, so that the moment the second flag opens is set to t = 0.

### 4.3.2 Oxygen desorption

Figure 4.6 shows TPD spectra that were collected after the KW experiments with incident energies of a) 0.056 eV, b) 0.23 eV, and c) 0.38 eV for various dosing surface temperatures. All TPD spectra of experiments at $T_s$ = 100 K (blue), show a desorption peak between 100 and 200 K ($\delta$-peak). This peak is due to molecular oxygen desorption and increases with increasing incident energy. The peak is absent when a surface temperature higher than 150 K was used. All TPD spectra show a broad desorption feature between $\sim$ 640 and 930 K, due to recombinative oxygen desorption ($\alpha$ and $\beta$-peaks). An additional, sharp feature ($\gamma$-peak) with a maximum between 670 and 684 K is visible for all energies at a dosing temperature of 100 K. This feature also develops with increasing $E_i$ and $T_s$. It is absent for all of the low energy TPD spectra between 200 (green) and 600 K (red). At high $E_i$, the $\gamma$-peak is observed for all dosing temperatures. The intensity is largest for 600 K and 100 K and lowest for 200 K.

We have compared the oxygen uptake curves from our KW experiments for $E_i$ = 0.056 eV and $T_s$ = 200 and 300 K to uptake curves from TPD experiments by Chang and Thiel[36] and Zheng and Altman[38] (only 335 K) (see Experimental). We have verified that adsorption via the KW experiments and desorption in the TPD experiments follow the same trend for the total obtained coverage. When we scale

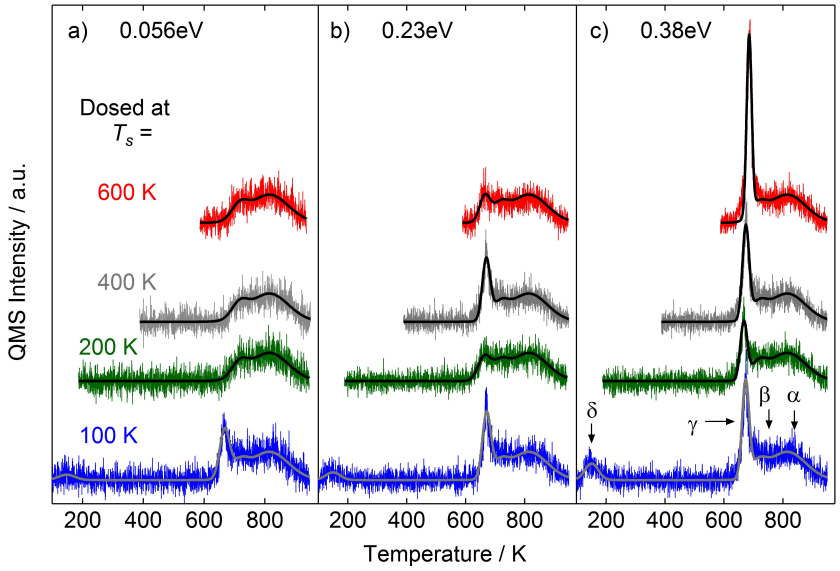


**Figure 4.6:** TPD spectra of mass 32 (including fits through the data), recorded after KW experiments with a) $E_i$ = 0.056 eV, b) 0.23 eV, and c) 0.38 eV for various $T_s$. The heating rate of the crystal is 2 K/s.

our KW uptake data to have a coverage of 0.34 ML, the uptake curves closely resemble those previously measured by TPD. Therefore, we assume that the total TPD desorption (combined $\alpha$ and $\beta$-peak) of $E_i$ = 0.056 eV and $T_s$ = 200 K adds up to 0.34 ML. We have applied this scaling factor to all of our TPD spectra.

The total oxygen coverage (total integrated TPD signal for the $\alpha, \beta, \gamma$, and $\delta$-peaks) as function of $E_i$ for various $T_s$ is shown in figure 4.7a. Note that in case our assumption of 0.34 ML for the combined $\alpha$ and $\beta$-peak is not correct, the data in the figure will shift along the y-axis. It does not affect the observed trends. The traces of 200 and 300 K and of 400 and 500 K are nearly identical. At the lowest two energies, the coverage does not change. At intermediate energies, the coverage increases with increasing energy. At high energy, the maximum obtained coverage saturates. At 600 K, the maximum coverage increases initially more slowly than for the other surface temperatures. Above 0.23 eV, it accelerates resulting in a maximum coverage of almost 0.6 ML at $T_s$ = 600 K and 0.38 eV. The maximum obtained coverage of the 100 K experiments is generally higher than the other surface temperatures. This additional oxygen is distributed over the $\gamma$ and $\delta$ peaks.

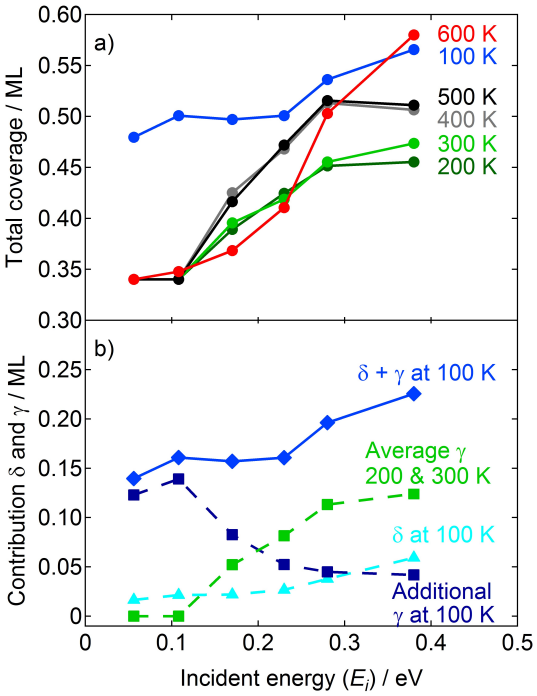


**Figure 4.7:** a) Integrated TPD peak areas of the total coverage ($\alpha$, $\beta$, $\gamma$ (and $\delta$)) in ML for oxygen desorption from Pd(100) as function of $E_i$ for various $T_s$ (circles). b) The average integral of the $\gamma$-peak for $T_s$ = 200 and 300 K (green squares), the $\delta$-peak at 100 K (triangles), and the additional $\gamma$-peak at 100 K (blue squares) compared to 200 and 300 K add up to the total contribution of the $\gamma$ and $\delta$-peak for $T_s$ = 100 K (diamonds).

Figure 4.7b shows a deconvolution of the amounts of desorbing $O_2$ in the different desorption features for the experiment performed at 100 K. The triangles show the amount of oxygen that desorbs in the $\delta$-peak. This may safely be assumed to result from desorption of molecularly adsorbed $O_2$. However, part of the molecular species present at 100 K may have dissociated during the temperature ramp instead of desorbing between 100 and 150 K. The dissociated fraction would reappear in the $\gamma$ peak. We estimate this contribution in the following way. The green squares indicate the average $\gamma$-peak of the experiments performed at 200 and 300 K. We assume that it is the same for the 100 K experiment for identical incident energy. The blue squares then reflect the amount of additional oxygen in the $\gamma$-peak as compared to the green squares. Hence the blue squares reflect our esti-

mate of molecular $O_2$ that dissociated instead of desorbed during the temperature ramp. The three dashed traces add up to the total amount of oxygen in the $\delta$ and $\gamma$-peak (diamonds) for experiment at 100 K. The ratio 'additional $\gamma$' to $\delta$ changes from 7.5 at low $E_i$ to 0.7 at high $E_i$. This ratio reflects a vastly changing tendency for molecular $O_2$ adsorbed on O-covered Pd(100) surface to dissociate vs. desorb.

The total obtained oxygen coverage on Pd(100) as determined from TPD traces as function of $E_i$ (horizontal axis) and $T_s$ (vertical axis) is shown in figure 4.8. This coverage plot was constructed from 36 averaged measurements (for 6 different temperatures and 6 different energies). The data is interpolated to show a more smooth transition between the data points. It clearly shows the higher coverage for the 100 K surface temperature for the entire energy range (orange/red). At high $E_i$ and high $T_s$, we also obtain a high surface coverage.

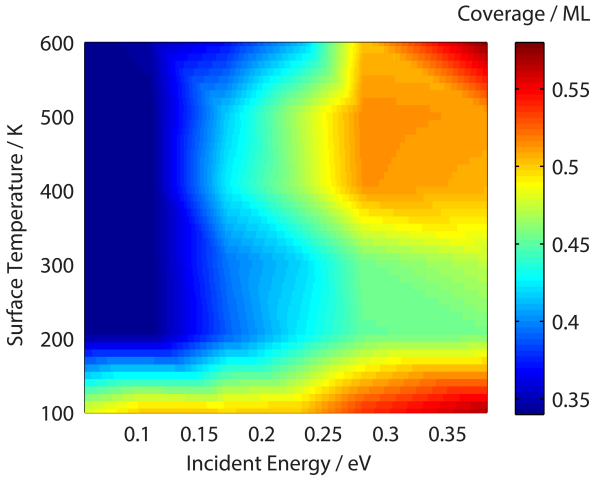


**Figure 4.8:** A surface plot of the total coverage in ML for oxygen desorption from Pd(100) as function of both incident energy (horizontal axis) and surface temperature (vertical axis).

Note that the total exposure used to obtain the data in figure 4.8 varies for different incident energies, but not for surface temperatures. The figure does not represent the obtained coverage per exposure, but the amount of $O_2$ detected during the subsequent desorption. Fluxes of the various $O_2$ beams vary non-linearly between the different kinetic energies by at most a factor of 1.8. As the TPD traces were taken after exposing the surface to a point where the sticking probability had dropped to (nearly) zero, exposures varying by this factor would not lead to signifi-

cant changes in the absolute coverage. Hence, the color-coding is neither skewed in either direction by experimental variations.

## 4.4 Discussion

### 4.4.1 Oxygen adsorption

The coverage-dependent sticking probability traces in figure 4.5 inform us on the adsorption dynamics of $O_2$ on the Pd(100) surface. The data for the lowest impact energy and lowest surface temperature show a nearly invariant sticking probability up to a point where it rapidly drops. Initially, the sticking probability actually even increases slightly, as it does for the 400 K trace. Such an independence on coverage or increase has been observed before for various systems[46,69,70]. It is often attributed to sticking via a precursor[54–56] state that has a long life time, suggesting that the molecule will find an adsorption site through diffusion, independent of where it originally impinged onto the surface. The precursor state may be located in the plane of the surface above an occupied site (extrinsic precursor) or above the bare surface (intrinsic precursor). However, sticking via such an equilibrated, mobile precursor seems not to be the case here.

First, a previous EELS study showed that the molecular oxygen state is not stable in the zero-coverage limit on Pd(100) at any of the temperatures in our experiments[33]. Hence, at least initially, molecular $O_2$ impinging onto the bare surface must dissociate. Sticking into a stable molecular state may only occur after sites are blocked by $O_2$ molecules that dissociated earlier. Second, we have shown previously that the weak kinetic energy dependence of initial sticking suggests that a direct dissociation process is dominant. Only at low incident energy it seems supplemented by a process that is sensitive to the molecular chemisorption well[71]. We referred to the latter as a dynamic precursor mechanism to dissociaiton to distinguish it from accommodated extrinsic or intrinsic precursor states. Such a dynamic precursor state is well-known for sticking of molecular hydrogen on stepped platinum surfaces[50,52,72,73].

Our coverage-dependent adsorption data support this view. From our TPD results, we can conclude that a molecular $O_2$ state must exist on the oxygen-covered surface and that it is occupied at high coverages in adsorption experiments performed with a surface temperature initially well below 200 K. At 150 K, we still

observe a small $\delta$-peak in TPD spectra, but at 200 K we do not. Although this molecular state must exist and can be occupied at higher coverages, the initial sticking coefficient and its rate of change in the first seconds of the adsorption experiments are identical for each set of incident energies. Exemplary data for 100 and 400 K are shown in figure 4.5. All other data for different conditions show the same behavior. The extent of the overlap of the traces varies per energy, but it lasts in each case long enough to account for a significant fraction of the total adsorbed oxygen. The absence of a surface temperature dependence in the dissociation probability in the first seconds strongly argues against sticking via any type of accommodated precursor state up to the coverage where the traces for 100 and 400 K deviate. Until the point of deviation is reached, a molecular state can therefore only be passed through transiently on the path to dissociation and can not be considered equilibrated. Beyond the point of deviation, molecular sticking into stable precursor states presents an additional mechanism at 100 K that is likely also related to the higher obtained final coverages apparent from the subsequent desorption experiments.

The insensitivity of the sticking probability on coverage for 100 K and 0.056 eV is thus not a result of dissociative sticking via equilibrated precursor states. It must result from consecutive adsorption mechanisms leading initially to dissociation and subsequently to additional molecular sticking. The necessary Langmuirian-like drop in time for sticking from the direct dissociative mechanism must be fully compensated by sticking into the molecular state. Hence, molecular sticking on partially O-covered Pd(100) is equally efficient as the initial dissociative sticking on the bare surface. This suggests that curvature of the potential leading into the molecular state is not strongly affected by occupancy of four-fold-hollow sites at or near the site of impact. The sudden drop in sticking in the trace indicates that this behavior is restricted to a certain limit and that molecular sticking reaches only a certain coverage on top of or in between the atomic states.

The difference between the 100 and 400 K traces may be interpreted as additional molecular sticking on partially O-covered Pd(100). The point at which traces for the different temperatures start deviating varies with kinetic energy. As fluxes for beams with different kinetic energies vary, the point at which deviation occurs in terms of flux or dissociated $O_2$ may not be directly obtained from figure 4.5. We will show elsewhere that the coverage-dependence observed for the intermediate energies can be quantitatively explained as a summation of the behaviors observed

for the lowest and highest incident energies.

As fluxes are not equal for experiments using various kinetic energies, the total integrated areas under the curves can also not be compared for the three panels in figure 4.5. Correcting for the different fluxes shows that the accumulated O-coverage in the adsorption experiments increases substantially with increasing kinetic energy. This is also reflected in figures 4.7 and 4.8, but then through the subsequent $O_2$ desorption. This effect is observed for any surface temperature.

Increasing maximum obtained coverages with increasing incident energies were also found for, e.g., $CH_4$ dissociation on Pt(111)[74]. It may imply that a new dissociation barrier in the entrance channel appears with increasing coverage or that an existing barrier shifts upward and/or toward the entrance channel of the potential energy surface. Considering that the invariant sticking at 100 K and 0.056 eV suggested no significant change in the entrance channel with increasing coverage, our data suggest that a modest barrier between the molecular and atomic state, i.e. in the exit channel, increases with coverage. It may still be overcome by additional kinetic energy of the impinging molecule. Recent DFT calculations report potential energy curves for $O_2$ binding to various O-covered Pd(100) surfaces[39]. Liu and Evans find that with increasing O-precoverage, the molecular state weakens while the barrier to dissociation increases. The binding energy of atomic states also decreases with coverage. This barrier is located in the exit channel. Hence, calculations and the interpretation of our experimental results are at least qualitatively in agreement.

Finally, it is noteworthy that in this picture of adsorption and dissociation for increasing coverage, the energy dependence on sticking indicates that the potential efficiently couples normal momentum of the impinging $O_2$ to lateral momentum of the individual nuclei, helping to surpass the rising dissociation barrier in the exit channel. This again argues against accommodation in a molecular precursor state for trajectories that end up in a dissociated state.

### 4.4.2 Oxygen desorption

To aid our understanding of Pd(100)'s oxygen uptake, we have divided the obtained coverage plot into various areas in figure 4.9. The arrows indicate the direction in which a higher surface coverage is obtained by independently varying incident kinetic energy or surface temperature.

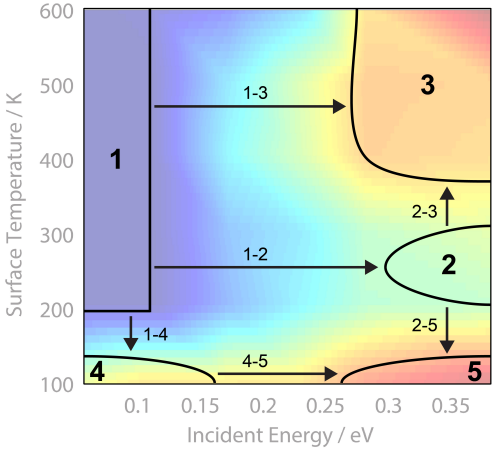


**Figure 4.9:** The maximum coverage of oxygen on Pd(100) is divided into five different areas that depend of incidence energy (horizontal axis) and surface temperature (vertical axis). The arrows indicate the pathways for obtaining a higher coverage.

Our starting point is area 1, where the coverage is relatively low. Above the surface temperature of 200 K, molecularly adsorbed $O_2$ is not stable and for the lower incident energies TPD spectra show the $\alpha$ and $\beta$-peaks only. The associated TPD area was scaled to a coverage of 0.34 ML as described previously. Although we can not distinguish surface structures by LEED, previous studies provide reference. The local coverages of the $p(2\times2)$ and $c(2\times2)$ structure, and the absence of the $\gamma$-peak for TPDs from area 1, require that the surface is composed of $p(2\times2)$ and $c(2\times2)$ patches with a ratio of roughly 2 : 1.

With increasing energy (areas 2 and 3), the $\gamma$-peak in TPD spectra appears whereas the subsequent $\alpha$ and $\beta$-peaks do not change. The sharp and narrow $\gamma$-peak has been observed before for adsorption at high surface temperatures[36,38,68]. The formation of this $\gamma$-peak is considered an activated process and indicates the presence of the $p(5\times5)$ and/or $(\sqrt{5}\times\sqrt{5})R27^\circ$ structures. The appearance of the peak in TPD spectra along line 1-2 shows that formation of these high coverage structures is indeed activated. The energetic barrier may be overcome by providing gaseous $O_2$ with more kinetic energy. This is interesting as formation of these structures not only involves dissociation of $O_2$, but also significant changes in the position of Pd atoms. This observation suggests that kinetic energy of $O_2$ is coupled rather efficiently to motion of other Pd and O atoms at the site of impact creating a

local high O-coverage PdO structure.

In region 2, the coverage approaches, but does not reach, 0.5 ML. As the $\gamma$-peak is present, adsorption can not solely have formed a nearly completed $c(2\times2)$ overlayer. Therefore, it must be a mix of three phases. The question then arises whether the high coverage phase was formed from highly energetic $O_2$ dissocation within the $p(2\times2)$ or $c(2\times2)$ patches, or at the boundaries between these. If only the former structure allows for additional dissociation, half of the $p(2\times2)$ area as obtained in area 1 needs to be converted to the the $p(5\times5)$ structure in area 2. If only the latter structure would allow for additional dissociation, the approximately 1/3 of the surface covered by $c(2\times2)$ in region 1 would have to be converted entirely into $(\sqrt{5}\times\sqrt{5})R27^\circ$, i.e. the structure with a highest local coverage near 0.8 ML to account for the TPD integral. This option seems less likely. Dissociation at boundaries between phases may also occur and initiate the formation of nuclei of the higher coverage PdO structures. Obviously, the total TPD integral may also be accounted for by a mix of these processes, i.e. additional dissociation on both $(2\times2)$ phases and their boundaries.

Surface temperature may also enhance the total oxygen uptake, similar to kinetic energy. Within region 1, no increase is observed in the obtained coverage over a 400 K span, whereas from region 2 the ultimate coverage rises from 0.45 ML to nearly 0.6 ML in region 3. The rise in coverage is associated with an increase in the $\gamma$-peak of desorption only. The thermal energy and kinetic energy variations in figure 4.9 are not quantitatively comparable though. Whereas thermal energy spans several tens of meV, the change in kinetic energy equals hundreds. Hence, we can not conclude that thermal energy is less effective in creating high coverage structures. On the other hand, the limited amount of additional thermal energy has a clear effect when kinetic energy is high. The increase along line 2-3 suggests that thermal energy aids in additional formation of the high coverage structures when they are initiated by high kinetic energy impact. Note that near 600 K, the high coverage structures also start to disintegrate. Hence, a possible interpretation of the topography of obtained surface coverage above 200 K is that kinetic energy facilitates nucleation of higher coverage PdO structures and that surface diffusion contributes to their growth. The size of various patches would then be governed by the kinetics of nucleation, growth, and disintegration of the PdO high coverage structures. If this interpretation is correct, an STM study in combination with oxidation by a supersonic molecular beam would show that two different sets

of conditions leading to the same overall coverage is associated with different distributions of patch sizes. The interpretation in terms of competing kinetics may also explain the delayed increase in the obtained coverage with kinetic energy for the 600 K trace as shown in figure 4.7a.

At adsorption temperatures between 100 and 150 K (areas 4 and 5), the molecular oxygen desorption peak ($\delta$-peak) and a $\gamma$-peak are observed in the subsequent TPD experiments. They account for the considerably higher coverages over the entire incident energy range as compared to surface temperatures ranging from 200 to 500 K. Following line 1-4 nearly 0.15 ML O adsorbs more at 100 K than at 200 K. At low kinetic energy, none of the high temperature experiments (area 1) show the $\gamma$-peak in figure 4.6. Therefore, the high coverage structure required to explain the $\gamma$ peak for area 4 is not formed while the surface is at 100 K. More likely, it is formed from dissociation of $O_2$ chemisorbed to the low coverage $p(2 \times 2)$ and/or $c(2 \times 2)$ structures. At low impact energy, these molecules adsorb to the abundant low atomic oxygen coverage areas and show preference for dissociation over desorption during the temperature ramp. When the kinetic energy is increased (line 4-5), higher coverage structures are already formed from direct dissociation. Consequentely, fewer $O_2$ molecules adsorb on top of this surface, and a preference for desorption over dissociation develops. These trends appear in figure 4.7b.

The appearance of the $\gamma$ peak for area 4 is quite surprising though. Nucleation of high coverage structures was ascribed to dissociation of molecules impinging with high kinetic energy. Thermal energy during the temperature ramp is low and would not be expected to assist much in overcoming the activation barrier to forming the high coverage PdO structures. However, if kinetic energy and the reaction energy are both easily absorbed locally by phonon excitations, and phonons drive the formation of the high coverage structures, the apparent contradiction is resolved. In other words, heating the surface does not generate the PdO nuclei, but deposition of energy from an impinging molecule creating a local hot spot does. A higher surface temperature then still contributes to growth of the PdO structures by increasing O diffusion. Recent dynamical calculations for $O_2$ dissociation on the Pd(100) surface support his idea. Phonon excitation to absorb the reaction energy is fast, efficient and local[42]. In the previous section we concluded that kinetic energy also seems to couple well to the surface.

## 4.5 Summary

The results of our adsorption and desorption experiments for $O_2$ on Pd(100) support the idea that dissociation is mostly direct. At low incident energy it may be supplemented by a dynamic precursor mechanism passing through a molecular state. At low surface temperatures and significant O-coverage this molecular state may be occupied. A chemisorbed $O_2$ molecule on (2x2)-type overlayers may also dissociate thermally and cause an unexpectedly high local coverage of a PdO-type structure. The formation of such high coverage structures is activated and can also be caused by kinetic energy of the impinging $O_2$ for surface temperatures where the molecular state is unstable. We suggest that the nucleation of PdO structures from the (2x2) structures with a local coverage exceeding 0.5 ML is induced by local phonon heating. These are excited efficiently by coupling of the reaction energy and kinetic energy of the impinging molecule to motion of Pd atoms at the site of impact. While locally-induced phonons drive the transition to PdO structures, thermal phonons aid in growing the PdO nuclei through increased diffusion of O atoms. The existence of the molecular state and the kinetics of nucleation, growth and decomposition of the high coverage structures cause an unexpected topography in oxygen adsorption as a function on incident energy and surface temperature.